Journal of Controlled Release 212 (2015) 94–102

Contents lists available at ScienceDirect

Journal of Controlled Release

journal homepage: www.elsevier.com/locate/jconrel

Enhancing cancer targeting and anticancer activity by a stimulus-sensitive multifunctional polymer-drug conjugate

Ying Tu, Lin Zhu *

Department of Pharmaceutical Sciences, Irma Lerma Rangel College of Pharmacy, Texas A&M University Health Science Center, Kingsville, TX 78363, United States

ARTICLE INFO

Article history:
Received 3 April 2015
Received in revised form 22 May 2015
Accepted 16 June 2015
Available online 22 June 2015

Keywords:
Drug delivery
Tumor targeting
Multifunctional
Matrix metalloproteinase 2
Cell penetrating peptide
Polymer-drug conjugate

ABSTRACT

Undesirable physicochemical properties, low tumor targeting, insufficient cell internalization, acquired drug resistance, and severe side effects significantly limit the applications of anticancer drugs. In this study, to improve the tumor targeting and drug efficacy of the poorly water-soluble drug, doxorubicin (DOX), a novel drug delivery platform (PEG-ppTAT-DOX) was developed, which contained a polyethylene glycol (PEG), a matrix metalloproteinase 2 (MMP2)-sensitive peptide linker (pp), a cell penetrating peptide (TAT), and a model drug (doxorubicin). The prepared drug platform possessed several key features, including: (i) the nanoparticle formation via the self-assembly; (ii) prevention of the non-specific interaction via the PEGylation; (iii) tumor targeting via the MMP2-mediated PEG deshielding and exposure of the TAT; (iv) the TAT-mediated cell internalization; (v) the TAT-induced endosomal escape; (vi) the inhibition of P-glycoprotein mediated drug efflux; and (vii) the TAT-medicated nuclear translocation. These cooperative functions ensured the improved tumor targetability, enhanced tumor cell internalization, improved intracellular distribution, and potentiated anticancer activity. Compared to the multi-component nanocarriers, the proposed simple but multifunctional polymer-drug conjugate might have greater potential for tumor-targeted drug delivery and enhanced chemotherapy.

1. Introduction

Chemotherapy is considered as one of the most effective approaches for treating human cancers. However, the severe drug-related side effects have limited the application of anticancer drugs. To decrease side effects, the cancer-specific therapies are preferred. Usually, the anticancer therapeutics are designed to recognize and bind to cancer cells via the cell surface receptors (known as the receptor-mediated tumor targeting) [1]. Although these strategies have improved the drug efficacy, the overall clinical outcomes remain unsatisfactory. Obviously, these strategies will not be effective when treating the cancer without well-defined cell surface receptors, like triple-negative breast cancer (TNBC) [2].

Matrix metalloproteinase (MMP) especially MMP2, is involved in the cancer growth, invasion, angiogenesis and metastasis and found up-regulated in many human cancers [3]. It has been used as a cancer biomarker and therapeutic target, and also provides a strategy for the on-demand delivery of drugs and imaging agents via an enzyme-triggered mechanism [4–6]. In our previous studies, the octapeptide (pp, GPLGIAGQ) sensitive to the human MMP2 was successfully used in drug nanocarriers including liposomes [4], polymeric micelles [5], and siRNA delivery nanocarriers [7] to improve tumor targetability. Compared to the receptor-mediated tumor targeting, the MMP2-sensitive strategy is cancer pan-specific and suitable for most types of cancers including the cancer without well-defined cell surface receptors.

Other undesirable properties, such as poor water solubility, insufficient cell internalization, and acquired drug resistance, also compromise the outcomes of anticancer drugs. Cell-penetrating peptides (CPPs) such as the trans-activating transcriptional activator (TAT) peptide have shown excellent membrane translocation capability and been widely used in drug nanocarriers and conjugates [4,5,8,9]. Among several possible mechanisms, the interaction between the positive charge of the TAT and the negative charge of the cell membrane plays an important role in the membrane translocation. The strategies, like PEGylation [4,5] or charge neutralization [6] have been used to prevent TAT-modified nanocarriers from the interaction with non-target tissues/cells and prolong their circulation time in bloodstream. However, various studies, including ours, showed that the protective PEG shell was not always beneficial for drug delivery. Ideally, the PEG should be deshielded before cell internalization [4,5,7].

To achieve an optimal clinical outcome of chemotherapy, all the issues associated with anticancer drugs have to be addressed. In this study, we proposed a simple but multifunctional polymer-drug conjugate system which contains a PEG, an MMP2-sensitive peptide linker (pp), a cell penetrating peptide (TAT), and a drug, for tumor targeted drug delivery. Using doxorubicin (DOX), a poorly water-soluble anthracycline, as a model drug, we developed a self-assembly polymer-drug conjugate,

* Corresponding author at: Department of Pharmaceutical Sciences, Irma Lerma Rangel College of Pharmacy, Texas A&M University Health Science Center, 1010 West Ave. B, MSC 131, Kingsville, Texas 78363, United States.
E-mail address: lzhu@tamhsc.edu (L. Zhu).

http://dx.doi.org/10.1016/j.jconrel.2015.06.024
0168-3659/

PEG-ppTAT-DOX, possessing multiple functions from its components to deal with the aforementioned challenges. Herein, the synthesis, purification, and characterization of PEG-ppTAT-DOX were described. The physicochemical properties and MMP2 sensitivity of the DOX conjugate were studied. Then, the cellular uptake, intracellular localization, drug efflux inhibition, anticancer activity, and apoptosis-inducing capability of the PEG-ppTAT-DOX were determined in various cancer cells including drug resistant cell lines.

2. Material and methods

2.1. Materials

Polyethylene glycol 2000-succinimidyl valerate ester (PEG2000-SVA) was from Laysan Bio (Arab, AL). Succinimidyl-4-(N-maleimidomethyl) cyclohexane-1-carboxylate (SMCC), chloroform, and acetonitrile were from Thermo Scientific (Rockford, IL). Dimethylformamide (DMF), triethylamine (TEA), and methanol were from Sigma-Aldrich Chemicals (St. Louis, MO). Human active MMP2 protein and analytical TLC plates were from EMD Biosciences (La Jolla, CA). Dialysis tubing (MWCO 2000 and 3500 Da) were from Spectrum Laboratories (Houston, TX). HEPES was from AMRESCO (Solon, OH). The preparative TLC plates were from Analtech (Newark, DE). Dulbecco's modified Eagle's medium (DMEM), penicillin streptomycin solution (PS) (100×), trypsin-EDTA, fetal bovine serum (FBS), and phosphate buffered saline (PBS) were from Mediatech (Manassas, VA). The doxorubicin (hydrochloride salt, >99%) was from LC Laboratories (Woburn, MA). The S Ceramic HyperD® F ion exchange column was from Pall Corporation (Port Washington, NY). Apo-ONE® Homogeneous Caspase-3/7 Assay kit was from Promega (Madison, WI). Annexin V-FITC Apoptosis Detection Kit I was from BD Biosciences (San Jose, CA). The mouse plasma (0.2 μm filtered) was from BioreclamationIVT (Baltimore, MD). Calcein AM was from Abcam Biochemicals (Cambridge, MA). The fluorescent mounting media was from Kirkegaard & Perry Laboratories (Gaithersburg, MD). Paraformaldehyde was from Alfa Aesar (Ward Hill, MA). Hoechst 33258 was from Enzo Life Sciences (Farmingdale, NY). The pp (GPLGIAGQ, >95%) was synthesized by Sigma Biosciences (Clarksburg, MD). The MMP2-sensitive cell penetrating peptide (ppTAT, GPLGIAGQYGRKKRRQRRRC, >95%) was synthesized by NeoBioLab (Woburn, MA).

The human non-small cell lung cancer (A549) cells (kindly provided by Dr. Narendra Kumar, Texas A&M Health Science Center), breast cancer (MCF-7), fibrosarcoma (HT1080), and the multi-drug resistant (MDR) ovarian cancer cells (NCI/ADR-RES) (kindly provided by Dr. Srinath Palakurthi, Texas A&M Health Science Center) were grown in complete growth media (DMEM supplemented with 1× PS and 10% FBS) at 37 °C in 5% CO_2 air.

2.2. Synthesis, purification and characterization of PEG-ppTAT-DOX

There are three steps in the synthesis of PEG-ppTAT-DOX. First, the MMP2-cleavable cell penetrating peptide (ppTAT) and PEG2000-SVA (1:1.1, molar ratio) were reacted in the carbonate buffer (pH 8.0) under nitrogen protection at 4 °C overnight, followed by the ion exchange chromatography to remove the excess PEG. The PEG-ppTAT was then desalted by the dialysis (MWCO 2000 Da) against water and checked by RP-HPLC as described previously [4]. Second, the maleimide group was conjugated to DOX via the reaction between doxorubicin hydrochloride (DOX HCl) and SMCC (1:1.2, molar ratio) in DMF containing 0.3% TEA in the dark at room temperature for 2 h. The DOX-SMCC was purified by the preparative TLC (chloroform:methanol:TEA, 80:20:0.3, v/v/v). Third, the PEG-ppTAT with a terminal cysteine was reacted with DOX-SMCC in DMF containing 0.3% TEA under nitrogen in the dark at room temperature overnight. The reaction was monitored by analytical TLC (chloroform: methanol, 80:20, v/v). The product was purified by preparative TLC and characterized by ^{1}H–nuclear magnetic resonance (NMR) spectroscopy on a Bruker 300 MHz spectroscope with deuterated methanol (CD_3OD) as a solvent. To check the fluorescence spectra, both the excitation and emission wavelengths of DOX or PEG-ppTAT-DOX were scanned on an Infinite® M1000 PRO microplate reader (Tecan).

2.3. Particle size and zeta potential

The particle size and zeta potential of PEG-ppTAT-DOX in PBS (0.5 mg/mL) were measured by dynamic light scattering (DLS) on a Particle Size and Zeta Potential Analyzer (NanoBrook 90Plus PALS, Brookhaven Instruments). To study the protein adsorption, the samples were mixed with the mouse plasma at 1/10 (v/v) and incubated at 37 °C in the dark for 0–4 h.

2.4. MMP2 sensitivity study

0.7 mM of the pp or ppTAT was incubated with the active human MMP2 in pH 7.4 HEPES buffered saline (HBS) containing 10 mM $CaCl_2$ at 37 °C overnight [5]. The cleavage of the peptides was analyzed on a Waters RP-HPLC system equipped with a C18 column. The chromatographic conditions were: solvent A—0.1% TFA in acetonitrile (ACN); solvent B—0.1% TFA in water. 0–15 min: 5%–75% A, 15–15.1 min: 75%–100% A, 15.1–20 min: 100% A, 20–20.1 min: 100%–5% A, and 20.1–25 min: 5% A. Flow rate: 1.0 mL/min at room temperature [4].

One mg/mL of the PEG-ppTAT-DOX was incubated with 6 ng/μL of the active human MMP2. Two methods were used to analyze the cleavage. For TLC, the samples were run in chloroform/methanol (8:2, v/v) followed by the Dragendorff's reagent staining to visualize the released PEG-peptide residue. For size exclusion chromatography (SEC), the digestion reaction mixture was applied on a Nanofilm SEC-250 SEC (7.8 × 50 mm, 5 μm) (Sepax Technologies, Inc.) at the flow rate of 0.4 mL/min of water and detected at 214 nm on a Waters HPLC system.

2.5. Cellular uptake study

To study the cellular uptake, the cells were seeded in 24-well plates at 1.0×10^5 cells/well. After overnight incubation, the cells were washed with pH 7.4 PBS and then incubated with DOX HCl or PEG-ppTAT-DOX in 300 μL/well of serum-free media. To study the influence of the MMP2, PEG-ppTAT-DOX was pre-incubated with human MMP2 overnight before adding to the cells. After incubation for 1 h or 2 h, the cells were washed with ice-cold PBS and analyzed by flow cytometry and fluorescence microscopy. For flow cytometry, the cells were trypsinized and collected by centrifugation at 2000 rpm for 4 min, followed by analysis on a BD Accuri C6 flow cytometer (BD Biosciences). The cells were gated upon acquisition using forward versus side scatter to exclude debris and dead cells. The data was collected (25,000 cell counts) and analyzed with Accuri CFlow Plus software. For fluorescence microscopy, the cells were washed by ice-cold PBS and the photos were taken with a Nikon Eclipse 80i fluorescence microscope.

2.6. Intracellular distribution study

The cells were seeded on glass coverslips in a 6-well plate at 4×10^5 cells/well and incubated overnight before treatment. The cells were incubated with DOX HCl or MMP2-pretreated PEG-ppTAT-DOX in 1 mL/well of serum-free media at 37 °C for 1 h. The coverslips were washed three times with PBS and then the cells were fixed with 4% paraformaldehyde for 5 min at room temperature. After washing with PBS, the cells were stained with 2 μg/mL Hoechst 33258 for 1 min. The coverslips were mounted onto microscope slides and analyzed by z-stack image acquisition with a step of 0.25 μm on a Nikon Eclipse Ti confocal microscope system at 1000×.

2.7. Calcein AM assay

To study the mechanism of the reversal of the drug resistance, the calcein AM [a common P-glycoprotein (P-gp) substrate] assay was performed. The 4×10^5 NCI-ADR/RES cells were grown in a 35 mm dish overnight before treatment. The cells were first incubated with PBS, PEG-ppTAT-DOX or MMP2-treated PEG-ppTAT-DOX at 0.3 μM at 37 °C for 30 min, and then incubated with 0.5 μM calcein AM for additional 30 min. The cells were washed with ice-cold PBS for three times, followed by fluorescence microscopy.

To quantitate the fluorescence intensity, the DOX or its conjugate was added into a 96-well plate. Then, 4×10^5 NCI-ADR/RES cells were added into the 96-well plate, and incubated at 37 °C for 20 min. Finally, 0.25 μM calcein AM were added to the wells, mixed and incubated for additional 20 min. To remove the extracellular calcein AM, the cells were washed three times by ice-cold PBS and collected by centrifugation at 200 *g* for 5 min. After lysing cells by DMSO, the fluorescence of the intracellular calcein AM was measured at $\lambda_{ex} = 494$ nm and $\lambda_{em} = 517$ nm.

2.8. Cytotoxicity study

To study the anticancer activity of PEG-ppTAT-DOX, the MMP2 overexpressing cells (A549 and HT1080), the cells without MMP2 overexpression (MCF7), and drug-resistant cells (NCI-ADR/RES) were grown at 5×10^3 cells/well in 96-well plates. The DOX HCl, PEG-ppTAT-DOX, or MMP2-treated PEG-ppTAT-DOX was incubated with the cells at various concentrations (0.03–200 μM) for 48 h in the complete growth medium, followed by the CellTiter-Blue® Cell Viability Assay. Briefly, 15 μL of the reagent was diluted with 100 μL of the complete growth medium per well and incubated with the cells at 37 °C for 2 h. Thereafter, the fluorescence intensity was recorded at $\lambda_{ex} = 560$ nm and $\lambda_{em} = 590$ nm on a microplate reader. The absolute half maximal inhibitory concentration (IC50) of each treatment was calculated. The toxicity of the PEG2000, ppTAT, and PEG-ppTAT was also evaluated in the A549 cells using the same protocol.

2.9. Apoptosis analysis

The A549 cells were grown in 24-well plates at 5×10^5 cells/well overnight before treatments. The cells were treated with DOX HCl or PEG-ppTAT-DOX at 1 μM for 48 h. Then the cells were trypsinized and washed with ice-cold PBS, followed by staining with 5 μL of Annexin V-FITC and 5 μL Propidium Iodide (PI) (FITC Annexin V Apoptosis Detection Kit I) for 15 min at room temperature in the dark. Then the cells were analyzed by flow cytometry.

2.10. Caspase 3/7 activation

The cells were grown in the 96-well plates at 5×10^3 cells/well overnight. Then, the cells were incubated with DOX HCl or PEG-ppTAT-DOX at 0.2 μM for 24 h, followed by the Apo-ONE® Homogeneous Caspase-3/7 Assay. Briefly, 50 μL of the reagent was added to each well containing 50 μL of cell media and incubated at room temperature for 1.5 h. Then, the fluorescence was measured on a microplate reader at $\lambda_{ex} = 485$ nm and $\lambda_{em} = 530$ nm.

2.11. Statistical analysis

Data were presented as mean ± standard deviation (SD) of triplicate. The difference of the groups was analyzed using a one-way ANOVA analysis. $P < 0.05$ was considered statistically significant.

3. Results and discussion

3.1. Design and synthesis of PEG-ppTAT-DOX

In our recent work, the combined use of the PEG, TAT peptide and the pp in the polymeric micelles has shown excellent tumor targeting and improved anticancer activity of the loaded drug [5]. In that study, these functional moieties were on different nanocarrier building blocks, which made the drug carrier complex. In the current study, to simplify the drug delivery system, a novel MMP2-sensitive cell penetrating peptide (ppTAT) (GPLGIAGQYGRKKRRQRRRC) containing both TAT and pp was used as a linker in the PEG-ppTAT-DOX. By this way, several drug delivery strategies, including the PEG-mediated long circulation, MMP2-sensitive peptide-mediated tumor targeting, and TAT-mediated cell internalization, were incorporated into one polymeric conjugate. The proposed mechanism of drug delivery is exhibited in Fig. 1.

The synthesis scheme of PEG-ppTAT-DOX is shown in the Fig. 2A. In our previous work, the PEGylated peptide has been successfully synthesized [5,7]. Here, the similar methods were used to synthesize PEG-ppTAT. To conjugate DOX to the PEG-ppTAT, the DOX was first maleimidated by the amine-to-sulfhydryl crosslinker, SMCC. Then, the DOX-SMCC was able to react with the cysteine of the PEG-ppTAT. After conjugation, the polarity of the DOX conjugate was increased, allowing the conjugate to stay at the starting point, while free DOX migrated to higher position in the TLC plate (Fig. 2B). In the ^{1}H–NMR (Fig. 2C), DOX was characterized by the peaks of $-CH_3$ protons (1.20 ppm), and $-CH_2-$ protons (1.93 and 2.06 ppm). PEG was characterized by the peak of $-CH_2CH_2O-$ protons (3.57 ppm). The ppTAT peptide was characterized by the peaks of $-CH_3$ protons (0.76–0.9 and 1.08 ppm) and –NCHCO– protons (4.50 ppm). The integration of the characteristic peaks showed that the molar ratio among PEG ($-CH_2CH_2O-$, 3.57 ppm, n = 45) (a), ppTAT (–NCHCO–, 4.50 ppm, n = 13) (b), and DOX ($-CH_3$, 1.20 ppm, n = 1) (c) was approximately 1:1:1. The theoretical content of DOX per conjugate was approximately 11 wt.% based on the theoretical molecular mass.

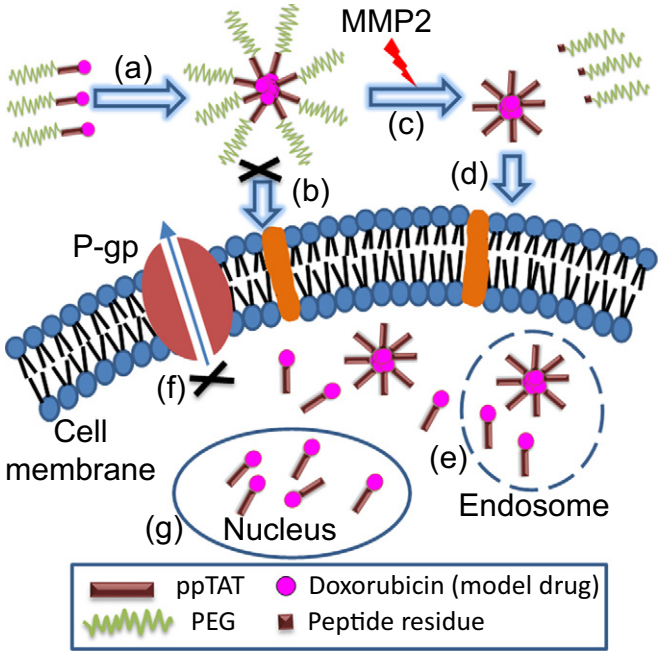

Fig. 1. Drug delivery mechanisms of PEG-ppTAT-DOX. Several strategies are used in PEG-ppTAT-DOX, including (a) the nanoparticle formation via the self-assembly; (b) prevention of the non-specific interaction with non-tumor cells via the PEGylation; (c) tumoral MMP2-mediated PEG deshielding and exposure of the TAT peptide; (d) the TAT-mediated cell internalization; (e) the TAT-induced endosomal escape; (f) the inhibition of P-gp mediated drug efflux; and (g) the TAT-medicated nuclear translocation.

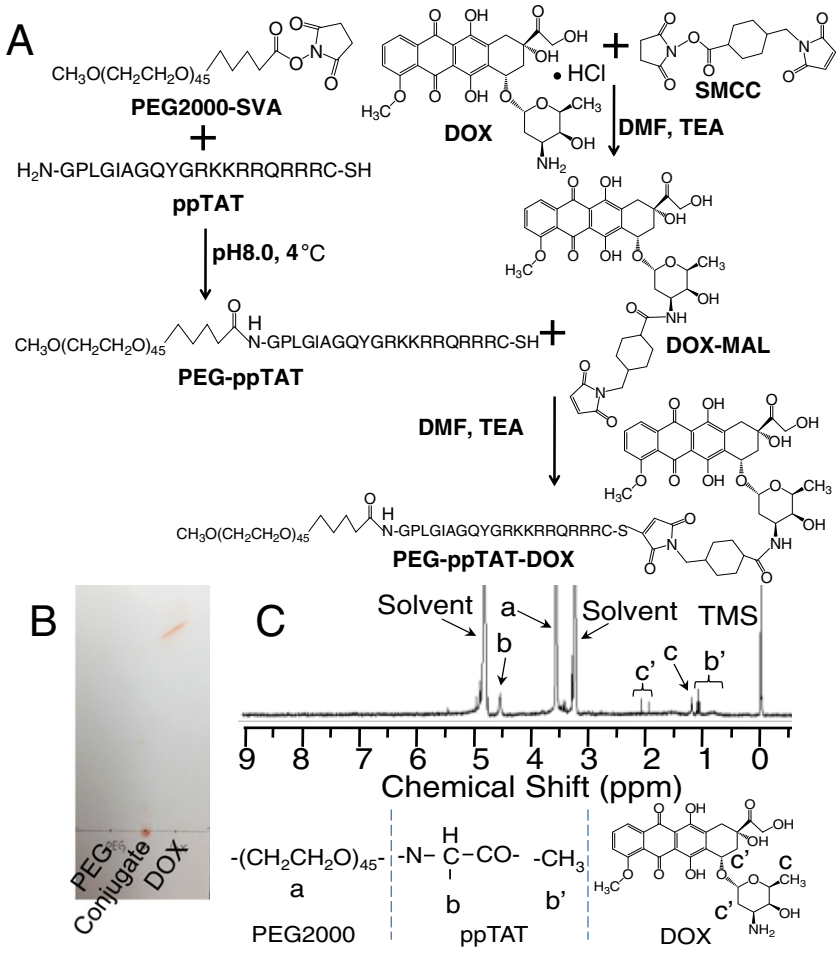

Fig. 2. (A) Synthesis scheme of PEG-ppTAT-DOX. (B) Thin layer chromatography (TLC). The samples were run and analyzed in the chloroform/methanol (7/3, v/v), no staining. PEG-ppTAT-DOX: 1 μg. (C) The ^{1}H–nuclear magnetic resonance (NMR) in CD_3OD.

According to the fluorescence spectra (Fig. 3A), the conjugation with PEG-ppTAT didn't significantly change the optical properties of the DOX, suggesting that the chemical and pharmacological properties of DOX were most likely retained after conjugation.

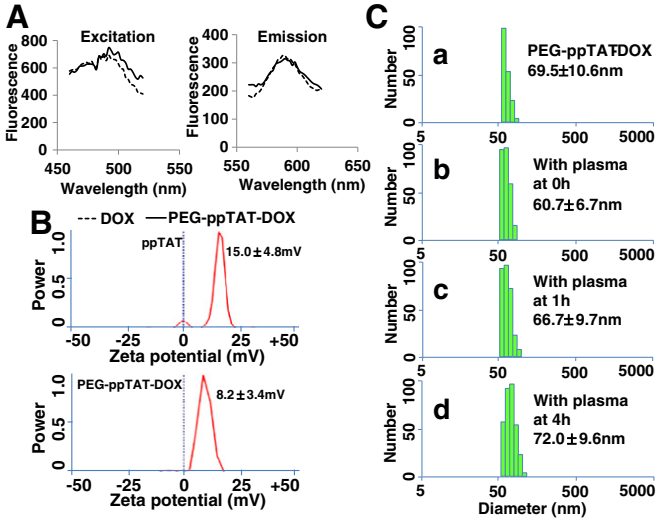

Fig. 3. (A) Fluorescence spectra of DOX and PEG-ppTAT-DOX. (B) Zeta potential of ppTAT peptide (upper panel) and PEG-ppTAT-DOX (lower panel) in PBS. (C) Particle size of PEG-ppTAT-DOX in PBS or with mouse plasma (1:10, v/v) at 37 °C for 0–4 h. a, PEG-ppTAT-DOX alone; b–d, PEG-ppTAT-DOX incubated with the mouse plasma.

3.2. Particle size and zeta potential

Free ppTAT had the zeta potential of around 15.0 ± 4.8 mV, while PEG-ppTAT-DOX had lower zeta potential of around 8.2 ± 3.4 mV (Fig. 3B). The data confirmed that the charge of the molecules including the TAT could be shielded via the PEGylation [7]. The data also suggested that the function of the TAT might be inhibited at least in part via the PEGylation, although the ionic interaction between TAT and the biological membrane is just one of its mechanisms of action. The stealth property of the PEG2000 is therefore used to decrease the drug's nonspecific interaction with biological molecules and prolong drug's blood circulation time.

Like other amphiphiles, the PEG-ppTAT-DOX could form a nanoparticle rather than be fully dissolved in the aqueous buffer due to the self-assembly, as evidenced by its particle size (69.5 ± 10.6 nm) (a, Fig. 3C). To evaluate the in vivo stability of PEG-ppTAT-DOX, the interaction between the DOX conjugate and blood proteins were determined. The data showed that no significant aggregates have been observed after incubation of the DOX conjugate with mouse plasma up to 4 h at 37 °C (b–d, Fig. 3C). The appropriate particle size and excellent stability suggested that PEG-ppTAT-DOX would be suitable for the in vivo drug delivery and passive tumor targeting via the enhanced permeability and retention (EPR) effect.

3.3. MMP2-mediated cleavage

Due to the excellent MMP2 sensitivity [5,7], the pp was used as an MMP2-sensitive moiety in the custom designed 20-amino acid peptide,

ppTAT. We found that the TAT didn't significantly influence the MMP2 sensitivity of the pp in the ppTAT, and both the pp and ppTAT showed the similar MMP2 sensitivity (Fig. 4A). The MMP2 sensitivity of PEG-ppTAT-DOX was also studied. In the TLC plate, a new spot with the migration rate close to that of free PEG was observed after the MMP2 incubation, indicating that the PEG could be deshielded, while the residue (IAGQ-TAT-DOX) was staying at the starting site due to its high polarity (Fig. 4B). In the SEC chromatogram, we also found that after digestion, the peak of the PEG-ppTAT-DOX was completely disappeared, while a new broad peak (digestion fragments) with longer retention time, similar to free PEG2000, was shown (Fig. 4C). These results suggested that PEG-ppTAT-DOX could be fully cleaved by the MMP2, resulting in the PEG deshielding.

3.4. In vitro cellular uptake

It has been reported that the conjugation of the functional peptides, such as MMP2-sensitive peptide or TAT peptide, to the hydrophobic drugs improved drug efficacy due to the increased solubility or cell internalization [8,10]. Therefore, we might hypothesize that the PEG-ppTAT-DOX containing the pp and TAT should possess the functions of both peptides. To verify the hypothesis, the cellular uptake study was performed in various cancer cell lines.

In the lung cancer (A549) cells, after 2 h incubation, the cellular uptake of the MMP2-pretreated PEG-ppTAT-DOX was about one-fold higher than that of the PEG-ppTAT-DOX (667% vs. 324%). The data indicated that the MMP2-mediated cleavage deshielded the PEG and exposed the TAT, resulting in the increase in the cellular uptake. The prolongation of the incubation time significantly increased the cellular uptake of both the DOX and MMP2-pretreated conjugate, while the conjugate without MMP2 pretreatment didn't show significant increase in its cell internalization (Figs. 5A and S1). The results were confirmed by the fluorescence microscopy, as evidenced by more red fluorescent cells after the MMP2 pretreatment (Fig. 5B).

To confirm the cellular uptake results, in addition to the lung cancer cells, the fibrosarcoma (HT1080), breast cancer (MCF7), and MDR ovarian cancer (NCI/ADR-RES) cells were also used as the in vitro cancer models. We found that free DOX was efficiently taken up by the drug-sensitive cells (A549, HT1080, and MCF7) but not drug-resistant NCI/ADR-RES cells (~350% vs. ~150%). The results confirmed the previous reports that the overexpressed P-gp of NCI/ADR-RES cells pumped out free DOX, one of the P-gp substrates [11]. In contrast, the cellular uptake of the MMP2-pretreated conjugate was more than 2-fold higher than those of free DOX in all tested cell lines (Fig. S2). It was noteworthy that the cellular uptake of the conjugate was the highest (>5-fold higher than that of free DOX) in the NCI/ADR-RES cells. The data suggested that PEG-ppTAT-DOX or its residue (IAGQ-TAT-DOX) might not be the substrates of the P-gp and could not be easily pumped out from the cells.

In the NCI/ADR-RES cells, we found that the MMP2-pretreatment led to more than 100% increase in the cellular uptake (2 h) of the conjugate. The prolongation of the incubation time from 1 h to 2 h didn't increase much in the cellular uptake of free DOX (134% vs. 146%) and the conjugate without MMP2-pretreatment (315% vs. 345%) (Figs. 5C and S3). The results were confirmed by the fluorescence microscopy (Fig. 5D). These data indicated that the PEG inhibited the interaction between the TAT and cell membrane, while upon the MMP2 cleavage, the exposed TAT enhanced the intracellular drug delivery in both drug-sensitive and -resistant cancer cells.

3.5. Intracellular distribution

It is well known that DOX has the nuclear targeting property. Our cellular uptake data have clearly showed that the DOX conjugate could enter cells much easier compared to free DOX. The intracellular distribution pattern of PEG-ppTAT-DOX would tell us if the conjugate had the same ability as the DOX. By confocal microscopy, after 1 h incubation, we found that both DOX and PEG-ppTAT-DOX (red) were co-localized with the cell nuclei (blue), and showed the pink fluorescence in the merged images. The co-localization was also clearly shown in the 3D image generated from the z-stack data. The red fluorescence in other intracellular compartments was very weak, indicating that PEG-ppTAT-DOX was not stuck in the endocytic vesicles and might undergo endosomal escape [12]. High nuclear accumulation of PEG-ppTAT-DOX was not only observed in the drug-sensitive HT-1080 cells but also in drug-resistant NCI/ADR-RES cells. These data suggested that, like DOX, PEG-ppTAT-DOX possessed the capability of nuclear targeting. Compared to free DOX, the PEG-ppTAT-DOX had higher level of drug nuclear translocation, as evidenced by stronger red fluorescence (Fig. 6). The possible reasons, here, might include (i) the increased intracellular concentration of DOX conjugates due to both the enhanced cellular uptake and decreased drug efflux; (ii) the TAT-mediated endosomal escape; and (iii) the increased binding affinity between the positively charged DOX conjugates (due to the conjugated TAT) and the negatively

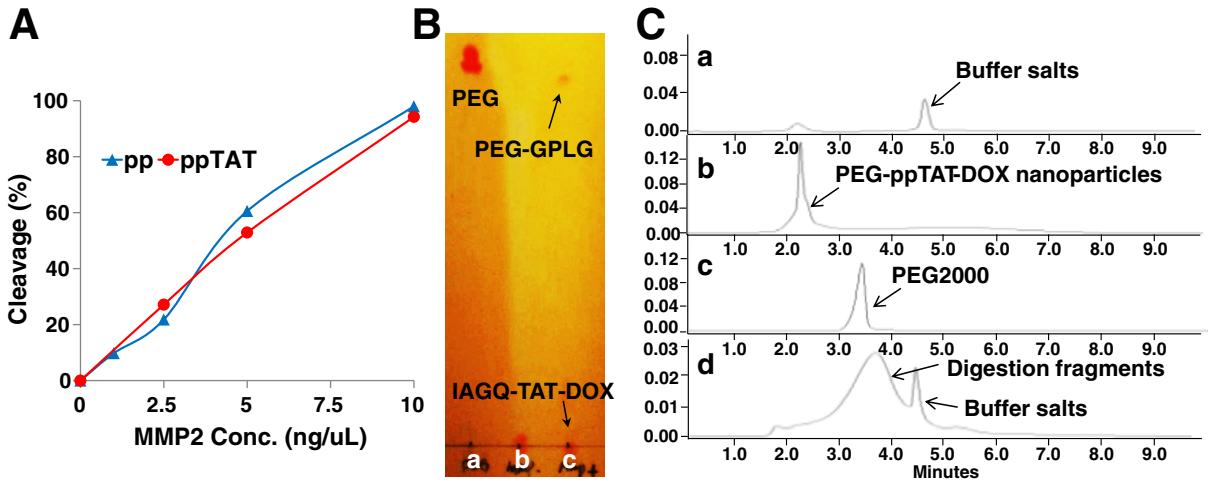

Fig. 4. MMP2 sensitivity study. (A) The cleavage of pp or ppTAT, quantitated by HPLC. (B) The cleavage of PEG-ppTAT-DOX analyzed by TLC (Dragendorff's reagent staining). a, PEG2000; b, PEG-ppTAT-DOX; c, MMP2-treated PEG-ppTAT-DOX. (C) The cleavage of PEG-ppTAT-DOX analyzed by the SEC. a, Digestion buffer; b, PEG-ppTAT-DOX in water; c, PEG2000 in water; d, MMP2-treated PEG-ppTAT-DOX in digestion buffer.

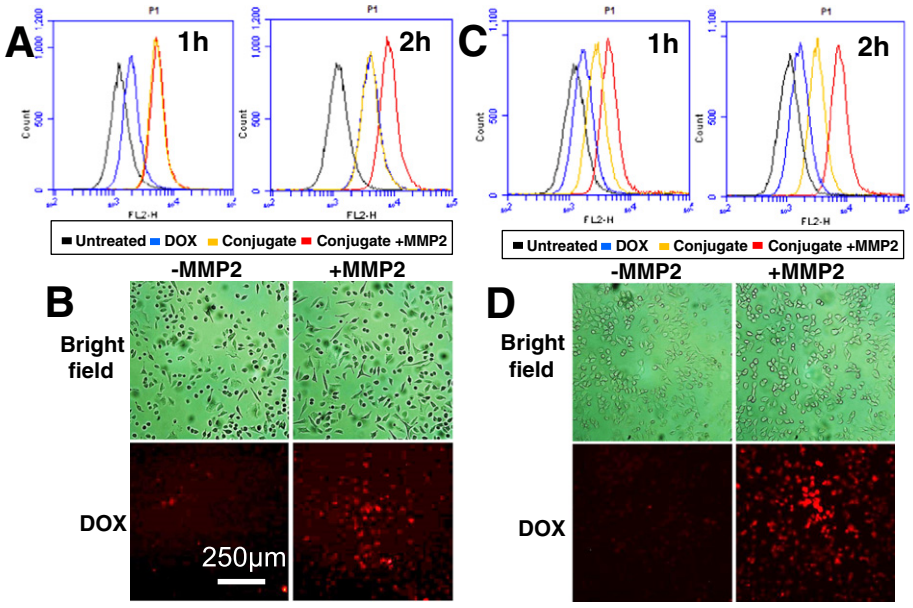

Fig. 5. The cellular uptake of the PEG-ppTAT-DOX in A549 (A and B) and NCI/ADR-RES (C and D) analyzed by the flow cytometry (upper panel) and fluorescence microscopy (lower panel). The cells were incubated with DOX or PEG-ppTAT-DOX for 1 h or 2 h. To study the influence of the MMP2, the conjugate was pre-incubated with human MMP2 overnight before adding to the cells.

charged DNA [13]. The improved intracellular distribution pattern (of the conjugate) would benefit the pharmacological effects of DOX.

3.6. P-gp inhibition

MDR is one of the major challenges of anticancer chemotherapy. Among many MDR mechanisms, the efflux of drugs due to the overexpression of MDR proteins, e.g. P-gp, is an essential step and found in almost all drug-resistant cancers [14]. To study if the PEG-ppTAT-DOX could influence the function of the P-gp, the cellular uptake of the calcein AM, a well-known fluorescent P-gp substrate, was performed. The short term incubation of NCI/ADR-RES cells with PEG-ppTAT-DOX significantly increased the intracellular concentration of calcein compared to the cells with PBS, as evidenced by strong green fluorescence (Fig. 7A). After quantitation, we found that the P-gp inhibition effect by PEG-ppTAT-DOX was dose-dependent (Fig. 7B). The data indicated that the PEG-ppTAT-DOX could influence the function of the P-gp and inhibit the efflux of not only itself but also other P-gp substrates. Here,

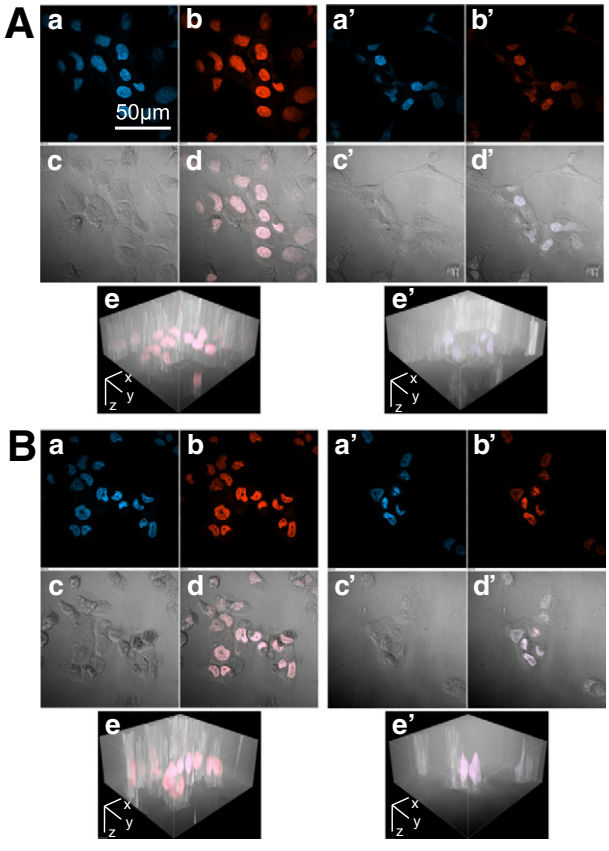

Fig. 6. The drug intracellular distribution in HT-1080 (A) and NCI/ADR-RES cells (B). The cells were incubated with DOX or MMP2-treated PEG-ppTAT-DOX for 1 h, followed by Hoechst 33258 staining before confocal microscopy. Left panel: PEG-ppTAT-DOX treated cells; right panel: DOX treated cells. a and a′, the Hoechst 33258 images; b and b′, the DOX images; c and c′, the differential interference contrast (DIC) images; d and d′, the merged images; e and e′, the 3D images generated from z-stack data.

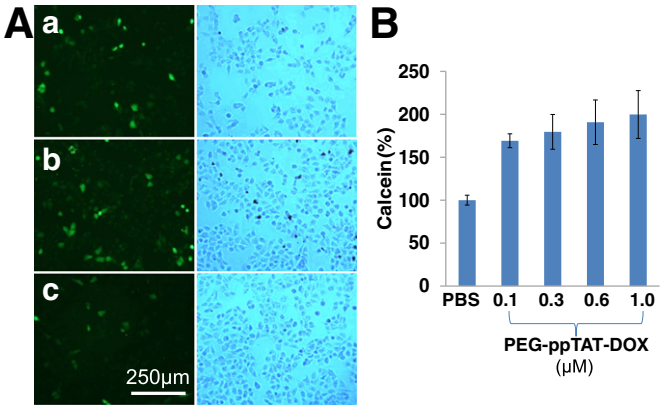

Fig. 7. Calcein AM Assay in the NCI-ADR/RES cells. (A) Fluorescence microscopy data. The cells were incubated with (a) PEG-ppTAT-DOX, (b) MMP2-pretreated PEG-ppTAT-DOX, or (c) PBS, followed by incubation with calcein AM. Left: fluorescent image; right: bright field. (B) Intracellular calcein intensity. The suspended cells were incubated with PBS or PEG-ppTAT-DOX, followed by incubation with calcein AM.

we postulated that PEG-ppTAT-DOX might have similar properties as those of the well-known polymeric P-gp inhibitors, Pluronic® block copolymers, in terms of anti-drug resistance [15]. However, to identify the mechanism behind, other P-gp substrates/drugs and more studies have to be done. The P-gp inhibition provided an opportunity for the future combined use of the PEG-ppTAT-DOX and other drugs for better anticancer effects.

3.7. In vitro anticancer activity

The anticancer activity of the conjugate was shown in Fig. 8A and Table 1. Compared to free DOX, the PEG-ppTAT-DOX showed comparable or lower cytotoxicity at low doses, while, interestingly, the DOX conjugate potentiated the drug efficacy at relatively high doses. It was probably because, at low doses, (i) the relatively slow drug release process delayed the action of the conjugated DOX [5], and (ii) the cleaved conjugate might not be as cytotoxic as the free DOX, while, at high doses, the TAT-mediated intracellular drug delivery, overwhelmed the process of the drug release and the lowered cytotoxicity. It has also been reported that, upon endocytosis, low endosomal pH could trigger the TAT insertion into the endosomal membrane and facilitate its translocation to the cytosol, so as to increase the cytosolic concentration of TAT-drug conjugates [12]. Moreover, the efficient nuclear translocation of the TAT peptide [13,16] might contribute to the improved drug efficacy since the intercalation with the DNA and stabilization of the topoisomerase II-DNA complexes are the major mechanisms of action of DOX [17]. These were confirmed by our intracellular distribution data (Fig. 6). Notably, the significant increase in the drug efficacy was not only observed in regular cancer cells but also in drug-resistant cells (a–d, Fig. 8A).

Table 1
The absolute IC50 (μM) of the DOX and DOX conjugates.

	A549	HT-1080	HT-1080 MCF-7	NCI/ADR-RES
DOX	0.50 ± 0.05	0.28 ± 0.04	0.47 ± 0.04	24.80 ± 6.58
PEG-ppTAT-DOX	1.06 ± 0.04	0.43 ± 0.01	1.14 ± 0.01	0.50 ± 0.03
PEG-ppTAT-DOX/MMP2	0.95 ± 0.05	0.36 ± 0.01	0.58 ± 0.04	0.42 ± 0.03

In the MMP2 overexpressing cells (HT-1080 and A549), the drug response curves (a and b, Fig. 8A) and IC50 (Table 1) between the PEG-ppTAT-DOX and its MMP2-pretreated counterpart were very similar. In contrast, the PEG-ppTAT-DOX had much less cytotoxicity compared to its MMP2-pretreated counterpart in the cells without MMP2 overexpression (MCF-7), as evidenced by a significant lag in the drug response curve (c, Fig. 8A) and a different IC50 (1.14 vs. 0.58 μM)

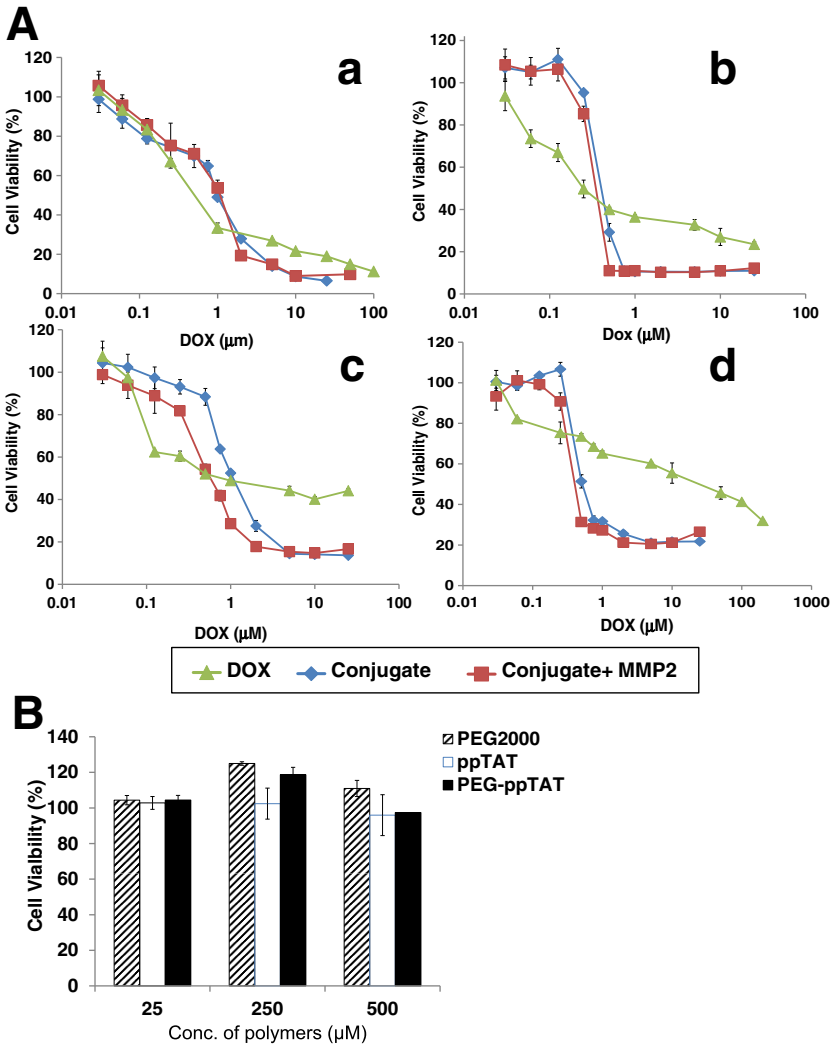

Fig. 8. (A) The cytotoxicity study of PEG-ppTAT-DOX in various cancer cell lines. The cancer cells were incubated with free DOX, PEG-ppTAT-DOX or MMP2-pretreated PEG-ppTAT-DOX in the complete growth medium for 48 h. The cell viability was determined by the CellTiter-Blue® Cell Viability Assay. a, A549 cells; b, HT-1080 cells; c, MCF-7 cells; d, NCI/ADR-RES cells. (B) The toxicity of the polymer and peptide used in the DOX conjugate. The cell viability was determined after 48 h incubation with the A549 cells.

(Table 1). These data indicated that, similar to the MMP2 pretreatment, the secreted MMP2 either in the cell medium [5] or on the cell surface [18] could efficiently cleave the pp, remove the PEG, and expose the TAT for the improved cellular uptake and intracellular distribution, resulting in the increased anticancer effect.

In the NCI/ADR-RES cells, free DOX only showed mild cytotoxicity with the IC50 of 24.8 μM compared to 0.5 μM in A549 cells, 0.28 μM in HT-1080 cells, and 0.47 μM in MCF-7 cells (Table 1), indicating that the significant drug efflux decreased the drug efficacy. Since PEG-ppTAT-DOX and free DOX had different cellular and intracellular properties, the IC50 might not be enough to evaluate the overall performance of the PEG-ppTAT-DOX. More aspects should be considered, such as the maximum effect (E_{max}) and slope, to give a comprehensive understanding of drugs' anticancer activity [19]. We found that the PEG-ppTAT-DOX could more efficiently bring down the E_{max} to around or less than 20% viability compared to the DOX in all cells, including drug-resistant cells, as evidenced by much steeper slopes in the drug response curves (Fig. 8A). Based on these data, we might say that PEG-ppTAT-DOX was more efficacious than free DOX although their IC50s were slightly lower than that of free DOX in regular cancer cells. The polymer and peptide alone didn't show any noticeable toxicity after 48 h incubation with A549 cells even at the concentration of up to 500 μM (Fig. 8B).

To study the apoptosis-inducing capability of the PEG-ppTAT-DOX, the cell apoptosis upon treatments were determined (Fig. 9A). After 48 h incubation with 1 μM DOX, most cancer cells underwent either apoptosis (PI negative, Annexin V positive) (47.2%) or death (both PI and Annexin V positive) (46.8%). Compared to DOX, the PEG-ppTAT-DOX caused similar level of apoptosis (47.3%) but less level of cell death (14.1%). These data were well consistent with the cytotoxicity data at the same dose (a, Fig. 8A). The caspase activity in the cancer cells was also measured. After 24 h incubation at 0.2 μM, both Dox and PEG-ppTAT-DOX activated the caspase pathway, as evidenced by about one fold increase in the caspase 3/7 activity (Fig. 9B). These results indicated that, like free DOX, the PEG-ppTAT-DOX could efficiently kill cancer cells via the induction of cell apoptosis. The conjugation with the PEG-ppTAT didn't change the mechanisms of action of the conjugated drug. However, the cell internalization and intracellular distribution of the PEG-ppTAT-DOX were significantly improved, resulting in the potentiated anticancer activity (Fig. 8A).

Altogether, the possible mechanisms for the improved efficacy of PEG-ppTAT-DOX might include: (i) the tumoral MMP2-mediated cleavage deshielded the PEG and exposed the TAT for better tumor targeting; (ii) the TAT enhanced cell internalization; (iii) the cell internalization via the P-gp independent pathway, e.g. endocytosis, bypassed the P-gp mediated drug efflux; (iv) the PEG-ppTAT-DOX inhibited the functions of the P-gp; (v) the TAT-mediated endosomal escape increased the cytosolic drug concentration; and (vi) the TAT-mediated nuclear translocation improved the accumulation of DOX in the cell nucleus and facilitated its action (Fig. 1).

Although some tumor cells, like MCF-7 cells, alone don't express MMP2, other cells in the tumor, e.g. the stromal cells [20] or macrophages [21], may be able to secret the MMP2 due to the cell–cell interaction in the tumor microenvironment. In addition to residing in tumor extracellular matrix (ECM), the secreted MMP2 can bind to the surface of cancer cells [18] and endothelial cells of blood vessels [22] to facilitate cancer cell's invasion and angiogenesis. Therefore, higher levels of tumoral MMP2 is expected in vivo [5]. Besides, the EPR effect also plays an important role in the tumor targeting when using nanoparticles [23]. Together with the current results, we may predict that, in the in vivo condition, PEG-ppTAT-DOX would have a better performance in terms of its tumor targeting and anticancer activity.

However, we also noticed that the PEG2000 could not fully shield the function of TAT moiety, as evidenced by the slight positive charge of PEG-ppTAT-DOX, and the moderate cellular uptake and cytotoxicity in the cells without MMP2 overexpression. From an in vivo point of view, to get a better tumor targeting, longer PEG or higher PEG density may be needed to completely block the function of the TAT [24,25]. The further optimization of the DOX conjugate and the in vivo evaluation are ongoing in our lab.

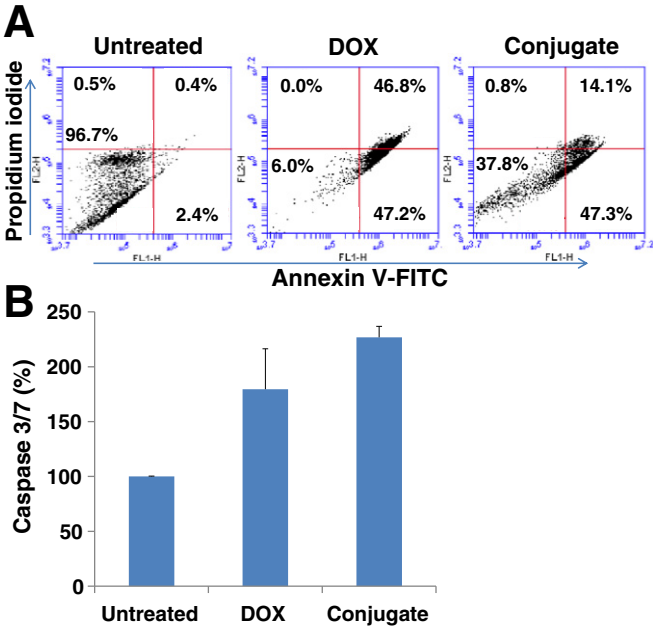

Fig. 9. Cell death and apoptosis. (A) Propidium iodide and annexin V-FITC double staining. The A549 cells were incubated with 1 μM DOX or its conjugate for 48 h. Then, the cells were stained by propidium iodide and annexin V-FITC, followed by flow cytometry. (B) Caspase 3/7 activity. The A549 cells were incubated with 0.2 μM DOX or its conjugate for 24 h, followed by the Apo-ONE® Homogeneous Caspase-3/7 Assay.

4. Conclusions

In the study, we prepared a simple but multifunctional drug platform, PEG-ppTAT-DOX, containing a PEG, an MMP2-sensitive cell penetrating peptide (ppTAT), and a model drug (DOX), for tumor-targeted drug delivery. The PEG-ppTAT-DOX showed the MMP2-mediated tumor targetability, the improved cell internalization and intracellular distribution, the P-gp inhibiting capability, and the potentiated anticancer efficacy in both drug sensitive and resistant cancer cells. Besides, due to its excellent self-assembly and stability in plasma, the PEG-ppTAT-DOX might be suitable for building other anticancer nanomedicine. The proposed drug platform showed great potential for the cancer-specific drug delivery.

Acknowledgments

Dr. Lin Zhu, the recipient of the Controlled Release Society (CRS) T. Nagai Postdoctoral Research Achievement Award, was partially supported by The Nagai Foundation Tokyo.

Appendix A. Supplementary data

Supplementary data to this article can be found online at http://dx.doi.org/10.1016/j.jconrel.2015.06.024.

References

[1] M. Scaltriti, J. Baselga, The epidermal growth factor receptor pathway: a model for targeted therapy, Clin. Cancer Res. 12 (2006) 5268–5272.
[2] S. Cleator, W. Heller, R.C. Coombes, Triple-negative breast cancer: therapeutic options, Lancet Oncol. 8 (2007) 235–244.
[3] M. Egeblad, Z. Werb, New functions for the matrix metalloproteinases in cancer progression, Nat. Rev. Cancer 2 (2002) 161–174.

[4] L. Zhu, P. Kate, V.P. Torchilin, Matrix metalloprotease 2-responsive multifunctional liposomal nanocarrier for enhanced tumor targeting, ACS Nano 6 (2012) 3491–3498.
[5] L. Zhu, T. Wang, F. Perche, A. Taigind, V.P. Torchilin, Enhanced anticancer activity of nanopreparation containing an MMP2-sensitive PEG-drug conjugate and cell-penetrating moiety, Proc. Natl. Acad. Sci. U. S. A. 110 (2013) 17047–17052.
[6] T. Jiang, E.S. Olson, Q.T. Nguyen, M. Roy, P.A. Jennings, R.Y. Tsien, Tumor imaging by means of proteolytic activation of cell-penetrating peptides, Proc. Natl. Acad. Sci. U. S. A. 101 (2004) 17867–17872.
[7] L. Zhu, F. Perche, T. Wang, V.P. Torchilin, Matrix metalloproteinase 2-sensitive multifunctional polymeric micelles for tumor-specific co-delivery of siRNA and hydrophobic drugs, Biomaterials 35 (2014) 4213–4222.
[8] J.F. Liang, V.C. Yang, Synthesis of doxorubicin-peptide conjugate with multidrug resistant tumor cell killing activity, Bioorg. Med. Chem. Lett. 15 (2005) 5071–5075.
[9] V.P. Torchilin, R. Rammohan, V. Weissig, T.S. Levchenko, TAT peptide on the surface of liposomes affords their efficient intracellular delivery even at low temperature and in the presence of metabolic inhibitors, Proc. Natl. Acad. Sci. U. S. A. 98 (2001) 8786–8791.
[10] R. Yamada, M.B. Kostova, R.K. Anchoori, S. Xu, N. Neamati, S.R. Khan, Biological evaluation of paclitaxel-peptide conjugates as a model for MMP2-targeted drug delivery, Cancer Biol. Ther. 9 (2010) 192–203.
[11] Y. Chen, S.R. Bathula, J. Li, L. Huang, Multifunctional nanoparticles delivering small interfering RNA and doxorubicin overcome drug resistance in cancer, J. Biol. Chem. 285 (2010) 22639–22650.
[12] H. Yezid, K. Konate, S. Debaisieux, A. Bonhoure, B. Beaumelle, Mechanism for HIV-1 Tat insertion into the endosome membrane, J. Biol. Chem. 284 (2009) 22736–22746.
[13] J.P. Richard, K. Melikov, E. Vives, C. Ramos, B. Verbeure, M.J. Gait, L.V. Chernomordik, B. Lebleu, Cell-penetrating peptides. A reevaluation of the mechanism of cellular uptake, J. Biol. Chem. 278 (2003) 585–590.
[14] G. Szakacs, J.K. Paterson, J.A. Ludwig, C. Booth-Genthe, M.M. Gottesman, Targeting multidrug resistance in cancer, Nat. Rev. Drug Discov. 5 (2006) 219–234.
[15] A.V. Kabanov, E.V. Batrakova, V.Y. Alakhov, Pluronic block copolymers for overcoming drug resistance in cancer, Adv. Drug Deliv. Rev. 54 (2002) 759–779.
[16] L. Pan, Q. He, J. Liu, Y. Chen, M. Ma, L. Zhang, J. Shi, Nuclear-targeted drug delivery of TAT peptide-conjugated monodisperse mesoporous silica nanoparticles, J. Am. Chem. Soc. 134 (2012) 5722–5725.
[17] D.A. Gewirtz, A critical evaluation of the mechanisms of action proposed for the antitumor effects of the anthracycline antibiotics adriamycin and daunorubicin, Biochem. Pharmacol. 57 (1999) 727–741.
[18] P.C. Brooks, S. Strömblad, L.C. Sanders, T.L. von Schalscha, R.T. Aimes, W.G. Stetler-Stevenson, J.P. Quigley, D.A. Cheresh, Localization of matrix metalloproteinase MMP-2 to the surface of invasive cells by interaction with integrin αvβ3, Cell 85 (1996) 683–693.
[19] M. Fallahi-Sichani, S. Honarnejad, L.M. Heiser, J.W. Gray, P.K. Sorger, Metrics other than potency reveal systematic variation in responses to cancer drugs, Nat. Chem. Biol. 9 (11) (2013) 708–714.
[20] C.F. Singer, N. Kronsteiner, E. Marton, M. Kubista, K.J. Cullen, K. Hirtenlehner, M. Seifert, E. Kubista, MMP-2 and MMP-9 expression in breast cancer-derived human fibroblasts is differentially regulated by stromal–epithelial interactions, Breast Cancer Res. Treat. 72 (2002) 69–77.
[21] T. Hagemann, S.C. Robinson, M. Schulz, L. Trumper, F.R. Balkwill, C. Binder, Enhanced invasiveness of breast cancer cell lines upon co-cultivation with macrophages is due to TNF-alpha dependent up-regulation of matrix metalloproteases, Carcinogenesis 25 (2004) 1543–1549.
[22] S.G. Kang, G. Zhou, P. Yang, Y. Liu, B. Sun, T. Huynh, H. Meng, L. Zhao, G. Xing, C. Chen, Y. Zhao, R. Zhou, Molecular mechanism of pancreatic tumor metastasis inhibition by Gd@C82(OH)22 and its implication for de novo design of nanomedicine, Proc. Natl. Acad. Sci. U. S. A. 109 (2012) 15431–15436.
[23] H. Maeda, The enhanced permeability and retention (EPR) effect in tumor vasculature: the key role of tumor-selective macromolecular drug targeting, Adv. Enzym. Regul. 41 (2001) 189–207.
[24] A. Mori, A.L. Klibanov, V.P. Torchilin, L. Huang, Influence of the steric barrier activity of amphipathic poly(ethyleneglycol) and ganglioside GM1 on the circulation time of liposomes and on the target binding of immunoliposomes in vivo, FEBS Lett. 284 (1991) 263–266.
[25] C.D. Walkey, J.B. Olsen, H. Guo, A. Emili, W.C. Chan, Nanoparticle size and surface chemistry determine serum protein adsorption and macrophage uptake, J. Am. Chem. Soc. 134 (2012) 2139–2147.